

AUTOMATED RETINAL LAYER SEGMENTATION AND THEIR THICKNESS PROFILES IN HEALTHY SUBJECTS

A Comparison of 55° Wide-field and Conventional 30° Spectral Domain-Optical Coherence Tomography

HELENA GIANNAKAKI-ZIMMERMANN, MD,*† MARION R. MUNK, MD, PhD,*†
ANDREAS EBNETER, MD, PhD,* SEBASTIAN WOLF, MD, PhD,*† MARTIN ZINKERNAGEL, MD, PhD*

Purpose: To assess whether retinal thickness measurements with a standard 30° spectral domain optical coherence tomography (SD-OCT) are comparable with wide-field 55° SD-OCT.

Methods: Thirty-three healthy individuals were scanned using 55° as well as 30° SD-OCT according to a standardized protocol. Automated retinal layer segmentation of standard and wide-field SD-OCTs was assessed using customized software.

Results: Both lenses showed a high correlation when analyzing total retinal thickness within the central, the inner, and the outer retinal ring ($r = > 0.9$). Automated thickness measurements with the 55° system were marginally higher compared with the 30° lens. The thickness of each separate retinal layer using automated segmentation showed excellent correlations within the inner and outer rings (range: $r = 0.6$ – $r = 0.9$ for the inner ring and range: $r = 0.9$ – $r = 1.0$ for the outer ring).

Conclusion: Fifty-five degree wide-field SD-OCT provides a good overview of the posterior pole and presents similar quantitative values as a standard 30° OCT lens. Therefore, thickness values are comparable when switching between these two lenses.

RETINA 40:2004–2009, 2020

Almost 2 decades ago, optical coherence tomography (OCT) has been introduced in clinical routine as a tool for retinal diagnostics. It has noninvasive properties and allows for two-dimensional imaging of the retina, analogous to the optical scattering from internal retinal tissue microstructures.¹ In diseases, in

which macular edema develops, for example, in diabetic maculopathy, measurements of the central retinal thickness are widely used to assess the course of macular disease or treatment response. Because of advances in automated retinal layer segmentation, there has been increasing interest in investigating individual retinal layers.^{2–6} Thinner inner retinal layers in the macular region were seen in patients with Type 2 diabetes even with only minimal diabetic retinopathy (DR) compared with controls.³ Furthermore, in patients with diabetes but without DR or with only incipient DR, a decreased retinal nerve fiber layer thickness and increased inner nuclear layer/outer plexiform layer thickness were detected. The outer retina remained unaffected at early stages of diabetes mellitus.⁴

In the clinical day-to-day life, follow-up examinations need to be precise and should allow a high degree of repeatability, to follow disease activity accurately and allow state-of-the-art treatment decisions in the daily routine as well as in clinical trials.

From the *Department of Ophthalmology, Inselspital, University Hospital Bern, Bern, Switzerland; and †Department of Ophthalmology, Inselspital, Bern Photographic Reading Center, University Hospital Bern, Bern, Switzerland.

Supported by a grant of the Swiss National Science Foundation (SNSF) (#320030_156019). The authors received nonfinancial support from Heidelberg Engineering GmbH (Heidelberg, Germany).

None of the authors has any conflicting interests to disclose.

This is an open-access article distributed under the terms of the Creative Commons Attribution-Non Commercial-No Derivatives License 4.0 (CCBY-NC-ND), where it is permissible to download and share the work provided it is properly cited. The work cannot be changed in any way or used commercially without permission from the journal.

Reprint requests: Helena Giannakaki-Zimmermann, MD, Department of Ophthalmology, Inselspital University Hospital, Universität Bern, CH-3010 Bern, Switzerland; e-mail: elena.gianna@gmail.com

A study of 2015 demonstrated exceptional repeatability and reproducibility of all eight retinal layer thickness measurements in young healthy subjects, using a new Spectralis spectral domain (SD)-OCT automatic segmentation software (software version 6.0; Heidelberg Engineering, Heidelberg, Germany).⁷

However, not only segmentation of the retinal layers but also the need for acquiring larger fields of the posterior pole using OCT—so called wide-field SD-OCT imaging—is of growing interest. Modern swept-source OCT technology, for example, showed that the extension of the scanning angle up to 100° in a single image is possible.⁸ This offers substantial advantages as it allows to image areas outside the temporal arcades and therefore may be useful for diagnosis and treatment decisions in various retinal conditions, ranging from retinal detachment to DR.⁹

Heidelberg Spectralis has recently introduced wide-field OCT imaging, with a 55° lens and a customized software. A previous study of our group already compared the performance of the 55° and the conventional 30° OCT in patients with diabetic macular edema (DME). This analysis revealed a strong interdevice agreement but also found that the wide-field OCT may be beneficial when evaluating the vitreomacular interface.¹⁰

In the current study, we investigated whether automated retinal layer segmentation of individual retinal layers using a 55° wide-field SD-OCT is comparable with the measurements using a standard 30° SD-OCT in a healthy cohort.

Methods

Patients and Setting

Ethics approval (KEK-Nr. 093/13) for this study was obtained from the local ethics committee, and the study was performed in accordance with International Conference on Harmonisation-Good Clinical Practice (ICH-GCP) guidelines and adhered to the tenets of the declaration of Helsinki.

This study included Spectralis 55° wide-field and standard 30° SD-OCTs of healthy volunteers. All SD-OCT images were acquired using the Spectralis SD-OCT (Heidelberg Engineering) system (Heidelberg Eye Explorer 1.9.10.0), and eyes were scanned using the 55° wide-field OCT module consisting of a 55° wide-field lens and a corresponding software as well as the standard Heidelberg 30° lens on the same day. Automated retinal layer segmentation of standard and wide-field SD-OCTs of 33 healthy subjects was performed using the inbuilt software. Individual retinal layer thickness was assessed according to the inbuilt

Early Treatment Diabetic Retinopathy Study subgrid. For statistical analyses, retinal thickness of all four inner and outer quadrants of each layer was averaged, and central retinal thickness was evaluated independently.

A standard scanning protocol was implemented. The horizontal area scanned (25°) and the distance between the scans (240 μ m) and the number of section scans (31) were equal for the 55° and the 30° volume scans, and only the vertical extension (30° vs. 55°) differed between both scanning patterns.¹⁰ Each scan was being averaged nine times. The 55° high-speed wide-field volume scan pattern thus consisted of a 55° \times 25° vertical raster scan, whereas the 30° high-speed volume scan pattern consisted of a 30° \times 25° vertical raster scan.

Before analysis was performed, the images were reviewed for alignment errors. In case of misalignment, the images were excluded from analyses, and the same was performed if automated segmentation failed.

Two representative images for the standard 30° and wide-field 55° SD-OCT are shown in Figure 1, A and B.

Only healthy eyes with a best-corrected visual acuity of 20/20 Snellen or more were included. Previous intraocular surgery was an exclusion criterion. Eyes with myopia of up to -4.0 dpt were accepted, whereas myopia of more than -4.0 dpt and hyperopia of more than $+2.0$ dpt were excluded. Subjects suffering from diabetes or arterial hypertension were excluded as well.

Only well-resolved raster scans were included for analysis with a minimum of 20-dB signal-to-noise ratio.¹¹

Statistical Analyses

Data analyses were performed using SPSS (IBM, SPSS statistics, Version 21; SPSS Inc, Chicago, IL) and Graph Pad Prism (GraphPad Software, Inc, La Jolla, CA). Given the normal distribution of the data, the concordance of the measurements between the conventional and the wide-field OCT were calculated using Pearson correlation and Spearman Rho correlation coefficient (r). P -values <0.05 were considered statistically significant. Values are given in mean \pm SD.

Results

This study included 33 eyes of 33 healthy volunteers (mean age 35 ± 10 years).

Agreement Between Conventional and Wide-Field OCT

No misalignment was found within the automated individual retinal layer segmentation for all included images.

To compare the two lenses, we analyzed the thickness of the central 1-mm ring, the 3-mm inner

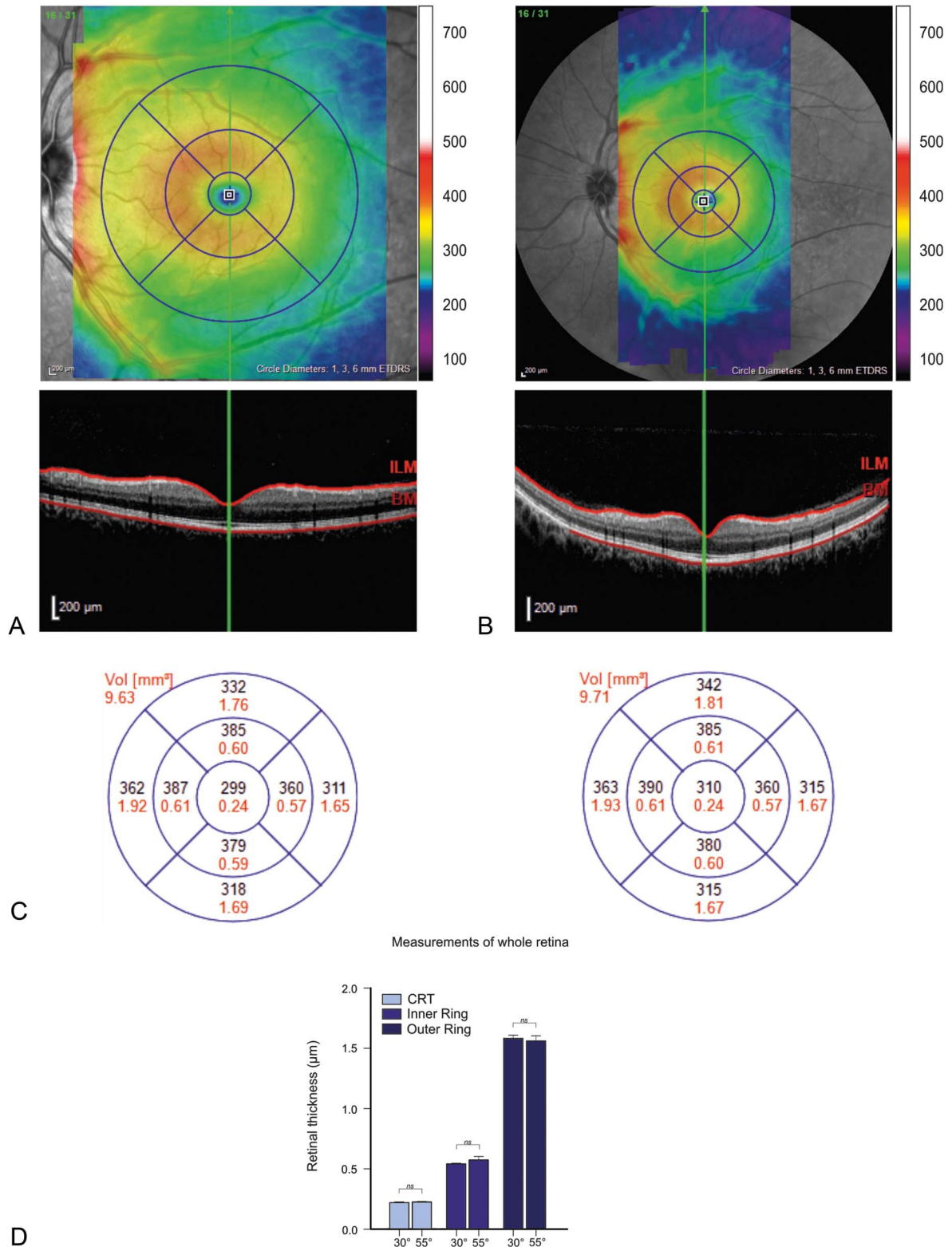


Fig. 1. Representative optical coherence tomography images of 30° and 55° degree vertical volume scans. Corresponding color-coded thickness maps with corresponding color scale in micrometers (μm) of 30° (**A**, top) and 55° (**B**, top) degree vertical volume scans with corresponding B scans (**A** and **B**, bottom) showing the boundaries of segmentation (red lines). **C.** Thickness maps of the 30° and the 55° degree lenses within the Early Treatment Diabetic Retinopathy Study quadrants (black; mean thickness in μm . red; mean volume in mm^3). **D.** Bar graphs of average retinal thickness for the center, the inner ring, and the outer ring. For each of these areas, the data of the 30° and of the 55° lens are shown ($n = 33$, paired t -test; $ns =$ not significant, $p < 0.05$ was considered statistically significant).

Table 1. Thickness measurements in volume (mm³) of the whole retina comparing the central ring, the inner ring, and the outer ring between the 30 degree and the 55 degree lens.

Whole Retina	30° Lens (Mean ± SD)	55° Lens (Mean ± SD)	r (Spearman Rho)
Central Ring	0.22 ± 0.02	0.22 ± 0.02	0.919*
Inner Ring	0.54 ± 0.03	0.57 ± 0.17	0.957*
Outer Ring	1.58 ± 0.17	1.56 ± 0.24	0.938*

*Correlation is significant at the 0.01 level. The last column shows how well the lenses correlate using Spearman Rho calculation.

ring, and the 6-mm outer ring. For the inner and outer ring analyses, the average of the four Early Treatment Diabetic Retinopathy Study quadrants (temporal, upper, nasal, and lower) was calculated. In a first step, we assessed the total retinal thickness and its ring compartments as described and correlated the data of the 30° lens with the results from the 55° lens.

We defined $r > 0.9$ as being a perfect or excellent correlation and a range $r = 0.6$ — $r = 0.9$ as a strong or good correlation.

A perfect agreement was found comparing thickness measurements of the total retina (central retinal thickness, inner, and outer retinal ring) between the two lenses ($r > 0.9$) (Table 1 and Figure 1), with a power of 0.95 for the current sample size of 33.

In a second step, we analyzed each individual retinal layer separately for the inner and outer ring. The individual layers of the central ring were not analyzed, as the retinal thickness of the central mm is mainly attributed to the outer nuclear layer (ONL). Strong correlation between the two lenses was found comparing each retinal layer separately within the inner ring (range; $r = 0.6$ — $r = 0.9$), and excellent correlation was found analyzing the outer ring (range: $r = 0.9$ — $r = 1.0$) (Tables 2 and 3).

In a third step, we compared relative thickness of individual layers obtained with the two lenses (Table 4) and found that the relative thicknesses were highly consistent between the two lenses.

Bland–Altman Plot Analysis

We also performed a Bland–Altman plot analysis to compare the two lenses and their thickness measurements (Figure 2).

The results show the agreement between retinal thickness measurements in the central area of the Early Treatment Diabetic Retinopathy Study grid, the inner ring, and the outer ring (95% limits of agreement from -0.14 to 0.01 for center, -0.016 to 0.015 for inner ring, and -0.04 to 0.02 for outer ring).

Discussion

In this study, we show that automated retinal layer segmentation with a wide-field 55° lens provides similar values as conventional 30° imaging. Data from total retinal thickness analysis revealed a nearly perfect correlation between the two lenses and as such can be used for follow-up analysis when switching from one lens to the other. Furthermore, our study shows a high correlation between automated segmentation of individual retinal layers when comparing the two lenses. Therefore, the bigger scan angle provided by the 55° lens offers a better overview of the entire macula without compromising accuracy of automated retinal layer segmentation. This could be useful for monitoring patients with diabetic macular edema or patients with larger pigment epithelial detachments in age-related macular degeneration (AMD) where conventional 30° imaging may be insufficient. Furthermore, wide-field OCT imaging has been shown to be superior for the assessment of the vitreomacular interface.¹⁰ However, despite these potential benefits, it was previously discussed that morphological alterations such as hard exudates may be missed using 55° wide-field imaging.¹⁰ This might be explained by the fact that there is a higher horizontal resolution of $11.74 \mu\text{m}/\text{pixel}$ in the conventional OCT scans using the high-speed mode

Table 2. Thickness measurements in volume (mm³) of the inner ring comparing each retinal layer separately between the 30 degree and the 55 degree lens.

Inner Ring	30° Lens (Mean ± SD)	55° Lens (Mean ± SD)	r (Spearman Rho)
RNFL	0.03 ± 0.0	0.04 ± 0.01	0.614*
GCL	0.08 ± 0.01	0.08 ± 0.01	0.638*
IPL	0.07 ± 0.01	0.06 ± 0.01	0.595*
INL	0.06 ± 0	0.06 ± 0.01	0.634*
OPL	0.05 ± 0.01	0.05 ± 0.01	0.644*
ONL	0.12 ± 0.02	0.12 ± 0.01	0.876*

*Correlation is significant at the 0.01 level. The last column shows how well the lenses correlate using Spearman Rho calculation.

Table 3. Thickness measurements in volume (mm³) of the outer ring comparing each retinal layer separately between the 30 degree and the 55 degree lens.

Outer Ring	30° Lens (Mean ± SD)	55° Lens (Mean ± SD)	r (Spearman Rho)
RNFL	0.19 ± 0.03	0.19 ± 0.04	0.890*
GCL	0.2 ± 0	0.2 ± 0.02	0.895*
IPL	0.16 ± 0.01	0.16 ± 0.01	0.899*
INL	0.18 ± 0.01	0.18 ± 0.01	0.853*
OPL	0.14 ± 0.01	0.15 ± 0.01	0.850*
ONL	0.32 ± 0.04	0.34 ± 0.08	0.969*

*Correlation is significant at the 0.01 level. The last column shows how well the lenses correlate using Spearman Rho calculation.

compared with 19.95 μm/pixel in the high-speed mode wide-field scans, which may impact the detectability of small lesions on OCT. However, the single scans may not always be on the exact same location of the retina, and therefore, a small, singular alteration may be missed on one of the scanning patterns.

The current study showed a very good agreement in terms of retinal thickness, central retinal thickness, and individual retinal layer results. However, we only analyzed healthy subjects, and so, we cannot exclude that results may differ when evaluating eyes with macular pathologies. In particular, an accurate automated segmentation of individual retinal layers may be much more challenging in these cases. Thus, in diseased eyes, discrepancies between individual retinal layer measurements, that is, due to segmentation errors may be possible. The fact that the retinal thickness results and the individual retinal layer results are comparable between the two lenses proves that the inbuilt automated segmentation of the 55° OCT works as accurate as the inbuilt automated segmentation of the conventional 30° OCT at least in healthy eyes. It remains to be shown, whether the segmentation algorithm of wide-field OCT is as accurate as the 30° algorithm in eyes with macular pathologies. A study from 2011 compared two different SD-OCT devices for their accuracy and reproducibility of retinal thickness measurements in exudative AMD, one of which was a Spectralis (Heidelberg Engineering) device. They found some differences in segmentation quality and reproducibility between the devices but also that manual correction of segmentation and manual scan reposition in case of decentered scans improved the

Table 4. Relative thickness of each individual retinal layer compared between the 30 degree and the 55 degree lens.

Retinal Layers	30° Lens (%)	55° Lens (%)
RNFL	12.43	12.77
GCL	15.68	15.43
IPL	13.51	12.77
INL	13.51	13.83
OPL	11.35	11.70
ONL	28.11	28.19
RPE	5.41	5.32

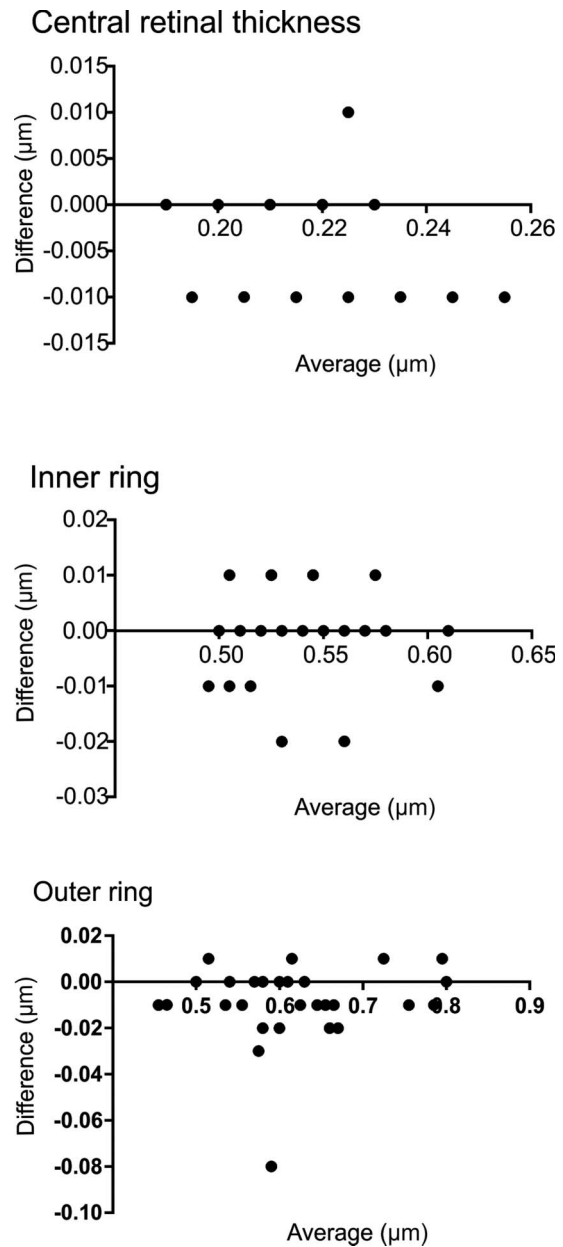


Fig. 2. Bland–Altman plot showing the agreement between retinal thickness measurements in the central area of the Early Treatment Diabetic Retinopathy Study grid, the inner ring, and the outer ring (95% limits of agreement from −0.14 to 0.01 for center, −0.016 to 0.015 for inner ring, and −0.04 to 0.02 for outer ring).

reproducibility.¹² This shows that automated evaluated retinal thickness values in retinal pathologies might reveal higher variability and lower concordance than in normal eyes among different devices/modules, and that automated segmentation seems more prone to misalignment in diseased eyes. However, to the best of our knowledge, a study comparing the conventional 30° lens and the 55° lens in patients with retinal diseases has not been performed so far.

Another limitation of the alternate use of 55° and 30° system may be that the scan location may differ from one acquisition to another as there is no follow-up compatibility between the two lenses, which limits the scan-to-scan comparison between two consecutive visits.

In conclusion, the 55° wide-field SD-OCT provides a good overview of the posterior pole and is comparable regarding retinal thickness measurements of a standard 30° OCT lens, but further studies are necessary to confirm its potential also in eyes with macular pathologies.

Key words: OCT, retina, wide-field imaging, segmentation.

Acknowledgments

The authors thank Heidelberg Engineering GmbH for providing technical assistance.

References

- Huang D, Swanson EA, Lin CP, et al. Optical coherence tomography. *Science* 1991;254:1178–1181.
- Tavares Ferreira J, Alves M, Dias-Santos A, et al. Retinal neurodegeneration in diabetic patients without diabetic retinopathy. *Invest Ophthalmol Vis Sci* 2016;57:6455–6460.
- van Dijk HW, Verbraak FD, Kok PH, et al. Early neurodegeneration in the retina of type 2 diabetic patients. *Invest Ophthalmol Vis Sci* 2012;53:2715–2719.
- Vujosevic S, Midena E. Retinal layers changes in human pre-clinical and early clinical diabetic retinopathy support early retinal neuronal and Müller cells alterations. *J Diabetes Res* 2013;2013:905058.
- Munk MR, Beck M, Kolb S, et al. Quantification of retinal layer thickness changes in acute macular neuroretinopathy. *Br J Ophthalmol* 2017;101:160–165.
- Beck M, Munk MR, Ebnetter A, et al. Retinal ganglion cell layer change in patients treated with anti-vascular endothelial growth factor for neovascular age-related macular degeneration. *Am J Ophthalmol* 2016;167:10–17.
- Ctori I, Huntjens B. Repeatability of foveal measurements using Spectralis optical coherence tomography segmentation software. *PLoS One* 2015;10:e0129005.
- Kolb JP, Klein T, Kufner CL, et al. Ultra-widefield retinal MHz-OCT imaging with up to 100 degrees viewing angle. *Biomed Opt Express* 2015;6:1534–1552.
- Carrai P, Pichi F, Bonsignore F, et al. Wide-field spectral domain-optical coherence tomography in central serous chorioretinopathy. *Int Ophthalmol* 2015;35:167–171.
- Munk MR, Lincke J, Giannakaki-Zimmermann H, et al. Comparison of 55 degrees wide-field spectral domain optical coherence tomography and conventional 30 degrees optical coherence tomography for the assessment of diabetic macular edema. *Ophthalmologica* 2017;237:145–152.
- Balasubramanian M, Bowd C, Vizzeri G, et al. Effect of image quality on tissue thickness measurements obtained with spectral domain-optical coherence tomography. *Opt Express* 2009;17:4019–4036.
- Krebs I, Smretschmig E, Moussa S, et al. Quality and reproducibility of retinal thickness measurements in two spectral-domain optical coherence tomography machines. *Invest Ophthalmol Vis Sci* 2011;52:6925–6933.